Optical Metrology. Kjell J. Gåsvik

ISBN: 0-470-84300-4

7
Moiré Methods. Triangulation

7.1 INTRODUCTION

Figure 3.2 is an illustration of two interfering plane waves. Let us look at the figure for what it really is, namely two gratings that lie in contact, with a small angle between the grating lines. As a result, we see a fringe pattern of much lower frequency than the individual gratings. This is an example of the moiré effect and the resulting fringes are called moiré fringes or a moiré pattern. Figures 3.4, 3.8 and 3.9 are examples of the same effect. The mathematical description of moiré patterns resulting from the superposition of sinusoidal gratings is the same as for interference patterns formed by electromagnetic waves. The moiré effect is therefore often termed mechanical interference. The main difference lies in the difference in wavelength which constitutes a factor of about 10^2 and greater.

The moiré effect can be observed in our everyday surroundings. Examples are folded fine-meshed curtains (moiré means watered silk), rails on each side of a bridge or staircase, nettings, etc.

Moiré as a measurement technique can be traced many years back. Today there is little left of the moiré effect, but techniques applying gratings and other type of fringes are widely used. In this chapter we go through the theory for superposition of gratings with special emphasis on the fringe projection technique. The chapter ends with a look at a triangulation probe.

7.2 SINUSOIDAL GRATINGS

Often, gratings applied in moiré methods are transparencies with transmittances given by a square-wave function. Instead of square-wave functions, we describe linear gratings by sinusoidal transmittances (reflectances) bearing in mind that all types of periodic gratings can be described as a sum of sinusoidal gratings. A sinusoidal grating of constant frequency is given by

$$t_1(x, y) = a + a\cos\left(\frac{2\pi}{p}x\right) \tag{7.1}$$

where p is the grating period and where $0 < a < \frac{1}{2}$. The principle behind measurement applications of gratings is that they in some way become phase modulated (see

Section 4.7). This means that the grating given by Equation (7.1) can be expressed as

$$t_2(x, y) = a + a \cos 2\pi \left(\frac{x}{p} + \psi(x) \right) \tag{7.2}$$

$\psi(x)$ is the modulation function and is equal to the displacement of the grating lines from its original position divided by the grating period

$$\psi(x) = \frac{u(x)}{p} \tag{7.3}$$

where $u(x)$ is the displacement.

When the two gratings given by Equations (7.1) and (7.2) are laid in contact, the resulting transmittance t becomes the product of the individual transmittances, viz.

$$\begin{aligned} t(x, y) &= t_1 t_2 \\ &= a^2 \left\{ 1 + \cos \frac{2\pi}{p} x + \cos 2\pi \left[\frac{x}{p} + \psi(x) \right] \right. \\ &\quad \left. + \frac{1}{2} \cos 2\pi \left[\frac{2x}{p} + \psi(x) \right] + \frac{1}{2} \cos 2\pi \psi(x) \right\} \end{aligned} \tag{7.4}$$

The first three terms represent the original gratings, the fourth term the second grating with doubled frequency, while the fifth term depends on the modulation function only. It is this term which describes the moiré pattern.

Another way of combining gratings is by addition (or subtraction). This is achieved by e.g. imaging the two gratings by double exposure onto the same negative. By addition we get

$$t(x, y) = t_1 + t_2 = 2a \left\{ 1 + \cos \pi \psi(x) \cos 2\pi \left[\frac{x}{p} + \frac{1}{2} \psi(x) \right] \right\} \tag{7.5}$$

Here we see that the term $\cos \pi \psi(x)$ describing the moiré fringes are amplitude modulating the original grating.

Both Equations (7.4) and (7.5) have a maximum resulting in a bright fringe whenever

$$\psi(x) = n, \quad \text{for} \quad n = 0, \pm 1, \pm 2, \pm 3, \ldots \tag{7.6}$$

and minima (dark fringes) whenever

$$\psi(x) = n + \tfrac{1}{2}, \quad \text{for} \quad n = 0, \pm 1, \pm 2, \pm 3, \ldots \tag{7.7}$$

Both grating t_1 and t_2 could be phase-modulated by modulation functions ψ_1 and ψ_2 respectively. Then $\psi(x)$ in Equations (7.6) and (7.7) has to be replaced by

$$\psi(x) = \psi_1(x) - \psi_2(x) \tag{7.8}$$

In both multiplication and addition (subtraction), the grating becomes demodulated (see Section 3.6.4) thereby getting a term depending solely on $\psi(x)$, describing the moiré

fringes. By using square wave (or other types) of gratings, the result will be completely analogous.

Below we shall find the relations between $\psi(x)$ (and $u(x)$) and the measuring parameters for the different applications.

7.3 MOIRÉ BETWEEN TWO ANGULARLY DISPLACED GRATINGS

The mathematical description of this case is the same as for two plane waves interfering under an angle α (see Section 3.4). When two gratings of transmittances t_1 and t_2 are laid in contact, the resulting transmittance is not equal to the sum $t_1 + t_2$ as in Section 3.4, but the product $t_1 \cdot t_2$. The result is, however, essentially the same, i.e. the gratings form a moiré pattern with interfringe distance (cf. Equation (3.21))

$$d = \frac{\mathrm{p}}{2 \sin \dfrac{\alpha}{2}} \tag{7.9}$$

This can be applied for measuring α by measurement of d.

7.4 MEASUREMENT OF IN-PLANE DEFORMATION AND STRAINS

When measuring in-plane deformations a grating is attached to the test surface. When the surface is deformed, the grating will follow the deformation and will therefore be given by Equation (7.2). The deformation $u(x)$ will be given directly from Equation (7.3):

$$u(x) = p\psi(x) \tag{7.10}$$

To obtain the moiré pattern, one may apply one of several methods (Post 1982; Sciammarella 1972, 1982):

(1) Place the reference grating with transmittance t_1 in contact with the model grating with transmittance t_2. The resulting intensity distribution then becomes proportional to the product $t_1 \cdot t_2$.

(2) Image the reference grating t_1 onto the model grating t_2. The resulting intensity then becomes proportional to the sum $t_1 + t_2$. This can also be done by forming the reference grating by means of interference between two plane coherent waves.

(3) Image the model grating t_2, and place the reference grating t_1 in the image plane. t_1 then of course has to be scaled according to the image magnification. The resulting intensity becomes proportional to $t_1 \cdot t_2$.

(4) Image the reference grating given by t_1 onto a photographic film and thereafter image the model grating given by t_2 after deformation onto another film. Then the two films are laid in contact. The result is $t_1 \cdot t_2$.

(5) Do the same as under (4) except that t_1 and t_2 are imaged onto the same negative by double exposure. The result is $t_1 + t_2$.

Other arrangements might also be possible. In applying methods (1), (3) and (4), the resulting intensity distribution is proportional to $t_1 \cdot t_2$ and therefore given by Equation (7.4) which can be written

$$I(x) = I_0 + I_1 \cos 2\pi \psi(x) + \text{terms of higher frequencies} \tag{7.11}$$

By using methods (2) and (5), the intensity distribution becomes equal to $t_1 + t_2$ and therefore given by Equation (7.5), which can be written

$$I(x) = I_0 + I_1 \cos \pi \psi(x) \cos \frac{2\pi x}{p} + \text{other terms} \tag{7.12}$$

We see that by using methods (1), (3) and (4) we essentially get a DC-term I_0, plus a term containing the modulation function. In methods (2) and (5) this last term amplitude modulates the original reference grating. When applying low-frequency gratings, all these methods may be sufficient for direct observation of the modulation function, i.e. the moiré fringes. When using high-frequency gratings, however, direct observation might be impossible due to the low contrast of the moiré fringes. This essentially means that the ratio I_1/I_0 in Equations (7.11) and (7.12) is very small. We then have the possibility of applying optical filtering (see Section 4.5). For methods (4) and (5), this can be accomplished by placing the negative into a standard optical filtering set-up. Optical filtering techniques can be incorporated directly into the set-up of methods (1) and (2) by using coherent light illumination and observing the moiré patterns in the first diffracted side orders. A particularly interesting method (belonging to method (2)) devised by Post (1971) is shown in Figure 7.1. Here the reference grating is formed by interference between a plane wave and its mirror image. The angle of incidence and grating period are adjusted so that the direction of the first diffracted side order coincides with the object surface normal. Experiments using model gratings of frequencies as high as 600 lines/mm have been reported by application of this method. To get sufficient amount of light into the first diffraction order one has to use phase-type gratings as the model grating. For the description of how to replicate fine diffraction gratings onto the object surface the reader is referred to the work of Post.

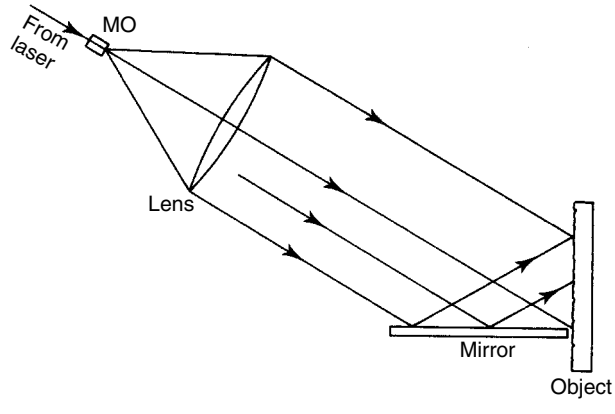

Figure 7.1

By using methods (3), (4) and (5) the grating frequency (i.e. the measuring sensitivity) is limited by the resolving power of the imaging lens. For curved surfaces, the model grating will be modulated due to the curvature, which can lead to false information about the deformation when using methods (1), (2) and (3). This is not the case for methods (4) and (5) because this modulation is incorporated in the reference grating (the first exposure). Surface curvature might also be a problem when using methods (3), (4) and (5) because of the limited depth of focus of the imaging lens. If we neglect the above-mentioned drawbacks, methods (1), (2) and (3) have the advantage of measuring the deformation in real time.

By using one of these methods, we will, either directly or by means of optical filtering, obtain an intensity distribution of the same form as given in the two first terms in Equation (7.11) or (7.12). This distribution has a

$$\text{maximum whenever } \psi(x) = n, \quad \text{for} \quad n = 0, 1, 2, \ldots$$

$$\text{minimum whenever } \psi(x) = n + \tfrac{1}{2}, \quad \text{for} \quad n = 0, 1, 2, \ldots$$

According to Equation (7.10) this corresponds to a displacement equal to

$$u(x) = np \quad \text{for maxima} \tag{7.13a}$$

$$u(x) = (n + \tfrac{1}{2})p \quad \text{for minima} \tag{7.13b}$$

Figure 7.2(a) shows an example of such an intensity distribution with the corresponding displacement and strain in Figures 7.2(b) and (c).

By orienting the model grating and the reference grating along the y-axis, we can in the same manner find the modulation function $\psi_y(y)$ and the displacement $v(y)$ in the y-direction. $\psi_x(x)$ and $\psi_y(y)$ can be detected simultaneously by applying crossed gratings, i.e. gratings of orthogonal lines in the x- and y-directions. Thus we also are able to calculate the strains

$$\varepsilon_x = p\frac{\partial \psi_x}{\partial x} \tag{7.14a}$$

$$\varepsilon_y = p\frac{\partial \psi_y}{\partial y} \tag{7.14b}$$

$$\gamma_{xy} = p\left[\frac{\partial \psi_x}{\partial y} + \frac{\partial \psi_y}{\partial x}\right] \tag{7.14c}$$

7.4.1 Methods for Increasing the Sensitivity

In many cases the sensitivity, i.e. the displacement per moiré fringe, may be too small. A lot of effort has therefore been put into increasing the sensitivity of the different moiré techniques (Gåsvik and Fourney 1986). The various amendments made to the solution of this problem can be grouped into three methods: fringe multiplication, fringe interpolation and mismatch.

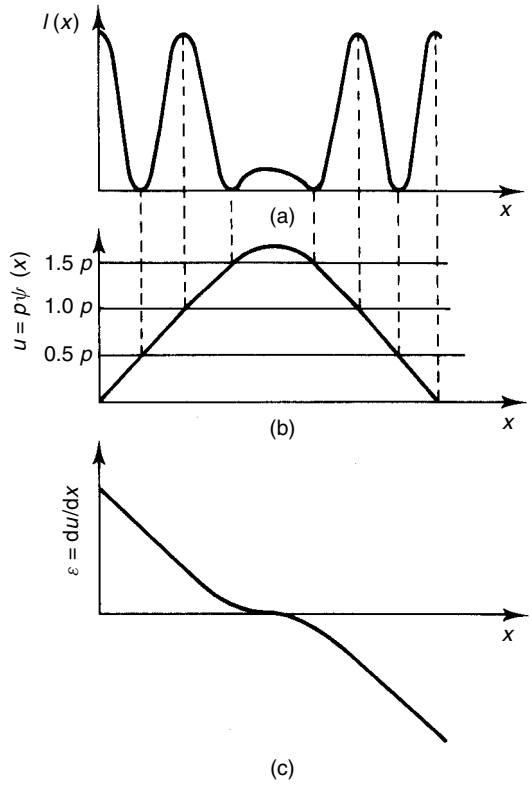

Figure 7.2 (a) Example of the intensity distribution of a moiré pattern with the corresponding; (b) displacement; and (c) strain

Fringe multiplication

In moiré methods one usually employs square-wave or phase gratings as model gratings. An analysis of such gratings would have resulted in expressions for the intensity distribution equivalent to Equations (7.11) and (7.12), but with an infinite number of terms containing frequencies which are integral multiples of the basic frequency. When using such gratings it is therefore possible to filter out one of the higher-order terms by means of optical filtering. By filtering out the Nth order, one obtains N times as many fringes and therefore an N-fold increase of the sensitivity compared to the standard technique. This is the concept of fringe multiplication. However, the intensity distribution of the harmonic terms generally decreases with increasing orders which therefore sets an upper bound to the multiplication process. Although in some special cases multiplications up to 30 have been reported, practical multiplications can rarely exceed 10.

Fringe interpolation

This method consists of determining fractional fringe orders. It can be done by scanning the fringe pattern with a slit detector or taking microdensitometer readings from

a photograph of the fringes. It can also be done by digitizing the video signal from a TV picture. These methods are limited by the unavoidable noise in the moiré patterns. When forming the reference grating by interference between two plane waves, interpolation can be achieved by moving the phase of one of the plane waves. This is easily obtained by means of e.g. a quarterwave plate and a rotatable polarizer in the beam of the plane wave.

For more details of such methods, see Chapter 11.

Mismatch

This is a term concerning many techniques. It consists of forming an initial moiré pattern between the model and reference grating before deformation. Instead of counting fringe orders due to the deformation, one measures the deviation or curvature of the initial pattern. The initial pattern can be produced by gratings having different frequencies, by a small rotation between the model and reference grating or by a small gap between them. In this way one can increase the sensitivity by at least a factor of 10.

This is equivalent to the spatial carrier method described in Section 11.4.3.

7.5 MEASUREMENT OF OUT-OF-PLANE DEFORMATIONS. CONTOURING

7.5.1 Shadow Moiré

We shall now describe an effect where moiré fringes are formed between a grating and its own shadow: so-called shadow moiré. The principle of the method is shown in Figure 7.3.

The grating lying over the curved surface is illuminated under the angle of incidence θ_1 (measured from the grating normal) and viewed under an angle θ_2. From the figure we see that a point P_0 on the grating is projected to a point P_1 on the surface which by viewing is projected to the point P_2 on the grating. This is equivalent to a displacement of the grating relative to its shadow equal to

$$u = u_1 + u_2 = h(x, y)(\tan\theta_1 + \tan\theta_2) \tag{7.15}$$

where $h(x, y)$ is the height difference between the grating and the point P_1 on the surface. In accordance with Equation (7.3), this corresponds to a modulation function

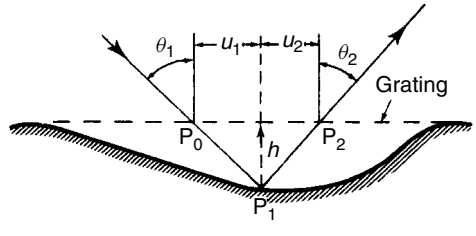

Figure 7.3 Shadow moiré

equal to

$$\psi(x) = \frac{u}{p} = \frac{h(x, y)}{p}(\tan\theta_1 + \tan\theta_2) \tag{7.16}$$

A bright fringe is obtained whenever $\psi(x) = n$, for $n = 0, 1, 2, \ldots$, which gives

$$h(x, y) = \frac{np}{\tan\theta_1 + \tan\theta_2} \tag{7.17a}$$

and

$$h(x, y) = \frac{(n + \frac{1}{2})p}{\tan\theta_1 + \tan\theta_2} \tag{7.17b}$$

for dark fringes. In this way, a topographic map is formed over the surface.

In the case of plane wave illumination and observation from infinity, θ_1 and θ_2 will remain constant across the surface and Equation (7.17) describes a contour map with a constant, fixed contour interval. With the point source and the viewing point at finite distances, θ_1 and θ_2 will vary across the surface resulting in a contour interval which is dependent on the surface coordinates. This is of course an unsatisfactory condition. However, if the point source and the viewing point are placed at equal heights z_p above the surface and if the surface height variations are negligible compared to z_p, then $\tan\theta_1 + \tan\theta_2$ will be constant across the surface resulting in a constant contour interval. This is a good solution, especially for large surface areas which are impossible to cover with a plane wave because of the limited aperture of the collimating lens.

If the surface height variations are large compared to the grating period, diffraction effects will occur, prohibiting a mere shadow of the grating to be cast on the surface. Shadow moiré is therefore best suited for rather coarse measurements on large surfaces. It is relatively simple to apply and the necessary equipment is quite inexpensive. It is a valuable tool in experimental mechanics and for measuring and controlling shapes.

Perhaps the most successful application of the shadow moiré method is in the area of medicine, such as the detection of scoliosis, a spinal disease which can be diagnozed by means of the asymmetry of the moiré fringes on the back of the body. Takasaki (1973, 1982) has worked extensively with shadow moiré for the measurement of the human body. He devised a grating made by stretching acrylic monofilament fibre on a frame using screws or pins as the pitch guide. According to him, the grating period should be 1.5–2.0 mm, and the diameter should be half the grating period. The grating should be sprayed black with high-quality dead back paint. Figure 7.4 shows an example of contouring of a mannequin of real size using shadow moiré.

7.5.2 Projected Fringes

We now describe a method where fringes are projected onto the test surface. Figure 7.5 shows fringes with an inter-fringe distance d projected onto the xy-plane under an angle θ_1 to the z-axis. The fringe period along the x-axis then becomes

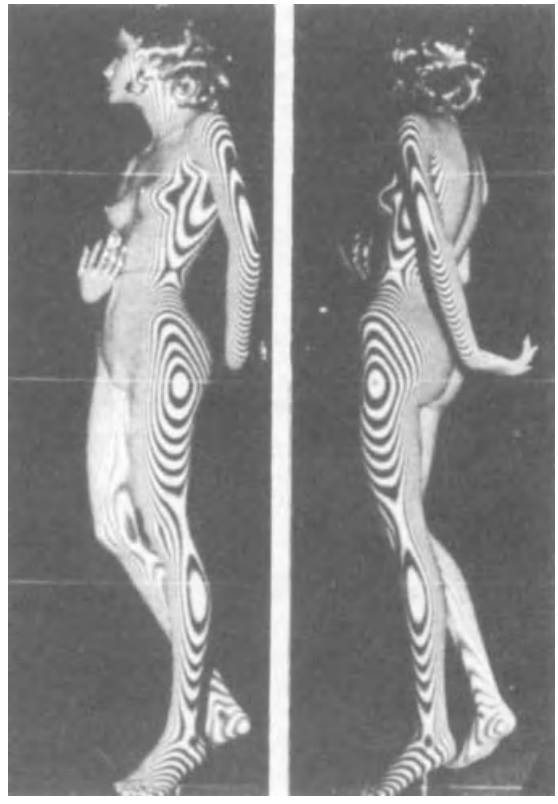

Figure 7.4 Shadow moiré contouring. (Reproduced from Takasaki 1973 by permission of Optical Society of America.)

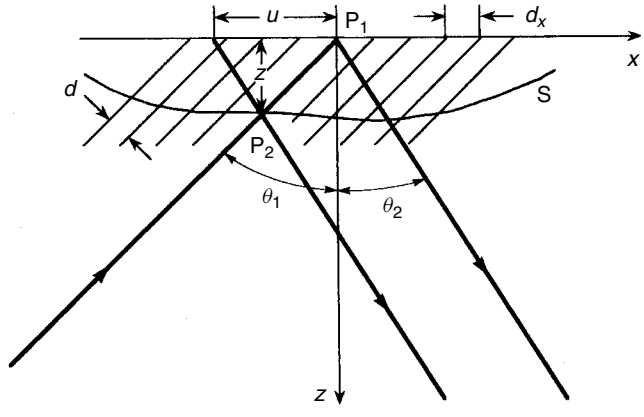

Figure 7.5 Fringe projection geometry. θ_1 = projection angle. θ_2 = viewing angle

$$d_x = \frac{d}{\cos\theta_1} \tag{7.18}$$

Also in the figure is drawn a curve S representing a surface to be contoured. From the figure we see that a fringe originally positioned at P_1 will be displaced to P_2. This displacement is given by

$$u = z(\tan\theta_1 + \tan\theta_2) \tag{7.19}$$

where z is the height of P_2 above the xy-plane and θ_2 is the viewing angle. From Equation (7.3) this gives a modulation function equal to

$$\psi(x) = \frac{u}{d_x} = \frac{z(\tan\theta_1 + \tan\theta_2)}{d/\cos\theta_1} = \frac{z}{d}(\sin\theta_1 + \cos\theta_1\tan\theta_2) = \frac{z}{d}\frac{\sin(\theta_1+\theta_2)}{\cos\theta_2} = \frac{z}{d}G \tag{7.20}$$

where we have introduced the geometry factor

$$G = G(\theta_1, \theta_2) = \sin\theta_1 + \cos\theta_1\tan\theta_2 = \frac{\sin(\theta_1+\theta_2)}{\cos\theta_2} \tag{7.21}$$

One method of projecting fringes on a surface is by means of interference between two plane waves inclined at a small angle α to each other. This can be achieved by means of a Twyman-Green interferometer with a small tilt of one of the mirrors (Figure 7.6(a)). The distance between the interference fringes is then equal to

$$d = \frac{\lambda}{2\sin(\alpha/2)} \tag{7.22}$$

where λ is the wavelength and α is the angle between the two plane waves.

From Equation (7.2) and Equations (7.18)–(7.21), the intensity distribution across the surface can then be written as

$$I = 2\left\{1 + \cos 2\pi\left[\frac{x}{d_x} + \psi(x)\right]\right\} = 2\left\{1 + \cos\frac{2\pi}{d}[x\cos\theta_1 + zG]\right\} \tag{7.23}$$

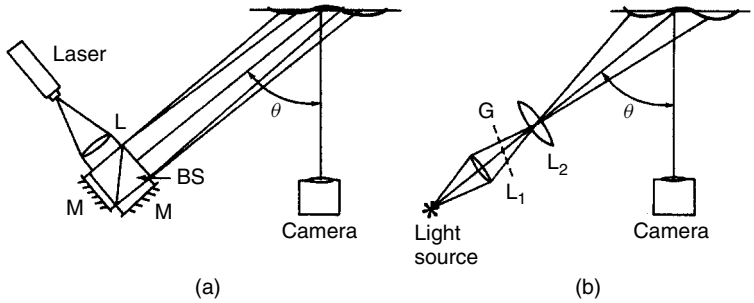

Figure 7.6 Fringe projection by means of (a) interference and (b) grating imaging. L = lenses, M = mirrors, BS = beamsplitter, G = grating

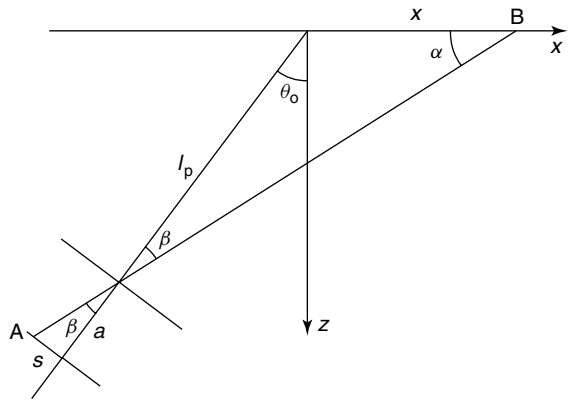

Figure 7.7 Grating projection

Figure 7.6(b) shows another method for projecting a fringe pattern onto the surface. Here, a grating is imaged onto the surface by means of a lens L_2. This situation can be analysed more closely from Figure 7.7 where a light ray through the centre of the projection lens goes from point A on the grating to point B on the xy-plane. A lies a distance s from the optical axis of the projection lens and B is a distance x from the origin of the coordinate system. From the figure we see that

$$\frac{x}{\sin\beta} = \frac{l_\mathrm{p}}{\sin\alpha} = \frac{l_\mathrm{p}}{\cos(\theta_\mathrm{o}+\beta)} = \frac{l_\mathrm{p}}{\cos\theta_\mathrm{o}\cos\beta - \sin\theta_\mathrm{o}\sin\beta} \tag{7.24}$$

which gives

$$\frac{x}{\tan\beta} = \frac{l_\mathrm{p}}{\cos\theta_\mathrm{o} - \tan\beta\sin\theta_\mathrm{o}} \tag{7.25}$$

where l_p is the distance from the lens to the origin of the coordinate system. By inserting

$$\tan\beta = s/a \tag{7.26}$$

where a is the grating–lens distance, we get

$$x = x(s) = \frac{s l_\mathrm{p}}{a\cos\theta_\mathrm{o} - s\sin\theta_\mathrm{o}} \tag{7.27}$$

Equation (7.27) gives the position $x = x(s)$ as a function of the position s on the grating. By increasing s by d_g, the grating period, we get for the fringe period d_x along the x-axis

$$d_x = x(s+d_\mathrm{g}) - x(s) = \frac{d_\mathrm{g} a l_\mathrm{p}\cos\theta_\mathrm{o}}{(a\cos\theta_\mathrm{o} - s\sin\theta_\mathrm{o})^2 - d_\mathrm{g}\sin\theta_\mathrm{o}(a\cos\theta_\mathrm{o} - s\sin\theta_\mathrm{o})} \tag{7.28}$$

In the following we approximate d_x/d_g by $\mathrm{d}x/\mathrm{d}s$, the derivative of x with respect to s:

$$\frac{d_x}{d_\mathrm{g}} \approx \frac{\mathrm{d}x}{\mathrm{d}s} = \frac{a l_\mathrm{p}\cos\theta_\mathrm{o}}{(a\cos\theta_\mathrm{o} - s\sin\theta_\mathrm{o})^2} \tag{7.29}$$

which we see is equal to Equation (7.28) when putting $d_g = 0$ in the denominator. This is a good approximation since d_g will be small compared to a. From Equation (7.27) we solve for s:

$$s = \frac{ax\cos\theta_o}{l_p + x\sin\theta_o} \tag{7.30}$$

which put into Equation (7.29) finally gives

$$d_x = \frac{d_g(l_p + x\sin\theta_o)^2}{al_p\cos\theta_o} = \frac{d_g l_p}{a\cos\theta_o}\left[1 + \frac{x\sin\theta_o}{l_p}\right]^2 = d_{xo}\left[1 + \frac{x\sin\theta_o}{l_p}\right]^2 \tag{7.31}$$

In the last equation we have introduced the quantity

$$d_{xo} = \frac{d_g}{\cos\theta_o}\frac{l_p}{a} \tag{7.32}$$

the fringe period for $x = 0$. When the grating is focused at $x = 0$, the projection magnification is

$$m_p = l_p/a \tag{7.33}$$

which gives

$$d_{xo} = m_p\frac{d_g}{\cos\theta_o} \tag{7.34}$$

For the instantaneous frequency we get

$$f_x = \frac{1}{d_x} = f_o\left[1 + \frac{x\sin\theta_o}{l_p}\right]^{-2} \tag{7.35}$$

where

$$f_o = \frac{1}{d_{xo}} = \frac{\cos\theta_o}{m_p d_g} \tag{7.36}$$

The phase along a line normal to the grating lines is given as s/d_g. We find the phase φ in the xy-plane from Equation (7.30):

$$\varphi = \frac{s}{d_g} = \frac{ax\cos\theta_0}{d_g(l_p + x\sin\theta_o)} = \frac{f_o x}{\left(1 + \dfrac{\sin\theta_o}{l_p}x\right)} \tag{7.37}$$

where f_o is given by Equation (7.36). The intensity in the xy-plane therefore can be written in the 'usual' way as

$$I(x, y) = A + B\cos 2\pi\varphi \tag{7.38}$$

with φ given from Equation (7.37). From the definition of the instantaneous frequency, we get

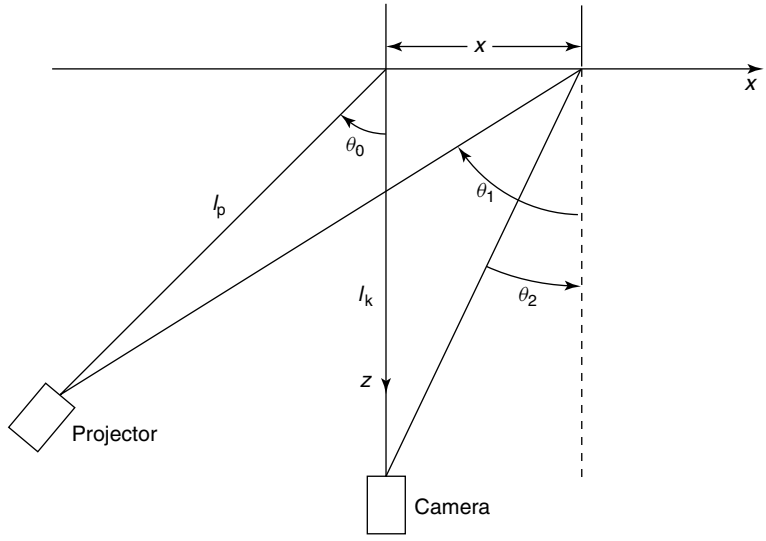

Figure 7.8 Fringe projection geometry

$$f_x = \frac{\mathrm{d}\phi}{\mathrm{d}x} = f_\mathrm{o}\left[1 + \frac{\sin\theta_\mathrm{o}}{l_\mathrm{p}}x\right]^{-2} \tag{7.39}$$

which agrees with Equation (7.35).

When the camera is pointing along the z-axis, we see from Figure 7.8 that

$$\tan\theta_1 = \frac{l_\mathrm{p}\sin\theta_\mathrm{o} + x}{l_\mathrm{p}\cos\theta_\mathrm{o}} \tag{7.40}$$

$$\tan\theta_2 = \frac{-x}{l_\mathrm{k}} \tag{7.41}$$

where θ_o is the projection angle measured from the z-axis and l_p and l_k are the projection and camera distances respectively. This gives for the displacement u and the phase ψ:

$$u(x) = z(\tan\theta_1 + \tan\theta_2) = \frac{z}{\cos\theta_\mathrm{o}}\left[\sin\theta_\mathrm{o} + \frac{(l_\mathrm{k} - l_\mathrm{p}\cos\theta_\mathrm{o})x}{l_\mathrm{p}l_\mathrm{k}}\right] \tag{7.42}$$

$$\psi(x) = \frac{u(x)}{d_x} = \frac{z}{d_{x\mathrm{o}}\cos\theta_\mathrm{o}}\left[\sin\theta_\mathrm{o} + \frac{(l_\mathrm{k} - l_\mathrm{p}\cos\theta_\mathrm{o})x}{l_\mathrm{p}l_\mathrm{k}}\right]\left[1 + \frac{x\sin\theta_\mathrm{o}}{l_\mathrm{p}}\right]^{-2} \tag{7.43}$$

From Equation (7.42) we see that the displacement u becomes dependent on x only through z (i.e. the contour interval becomes independent of the position on the surface) if the projection lens and the camera lens are placed at equal heights above the xy-plane ($l_\mathrm{k} - l_\mathrm{p}\cos\theta_\mathrm{o} = 0$).

Note that in general (from Equation (7.31)) the fringe period d_x is not constant but depends on x. The phase $\psi(x)$ given by Equation (7.43) therefore becomes more and more prone to error as the displacement $u(x)$ exceeds d_x with a factor much greater

than 1. This can, however, be solved by dividing by a sum of d_x in the right direction from the evaluation point. By inverting Equations (7.42) and (7.43) we get

$$z(x) = \cos\theta_o \left[\sin\theta_o + \frac{(l_k - l_p \cos\theta_o)x}{l_p l_k} \right]^{-1} u(x) \tag{7.44}$$

$$z(x) = d_{xo} \cos\theta_o \left[\sin\theta_o + \frac{(l_k - l_p \cos\theta_o)x}{l_p l_k} \right]^{-1} \left[1 + \frac{x \sin\theta_o}{l_p} \right]^2 \psi(x) \tag{7.45}$$

7.5.3 Vibration Analysis

In the same manner as for holographic interferometry, moiré technique using projected fringes (or shadow moiré) can be applied for vibration analysis of surfaces (Hazell and Niven 1968; Vest and Sweeney 1972; Harding and Harris 1983). Let us analyse this method more closely.

Assume that a point on the surface in Figure 7.5 executes harmonic out-of-plane vibrations given by

$$z = z_0 + a \cos\omega t \tag{7.46}$$

where z_0 is the equilibrium position, a is the amplitude and ω the frequency.

The intensity distribution of the projected pattern (cf. Equation (7.23)) now becomes

$$I(x,t) = 2\left[1 + \cos\frac{2\pi}{d}(x\cos\theta + (z_0 + a\cos\omega t)\sin\theta) \right] \tag{7.47}$$

where we for simplicity have assumed that the camera is imaging from infinity along the z-axis, i.e. $G = \sin\theta$ where θ is the projection angle.

The expression can be written as

$$I(x,t) = 2[1 + \cos(\phi_c + \phi_t)] = 2 + e^{i(\phi_c+\phi_t)} + e^{-i(\phi_c+\phi_t)} \tag{7.48}$$

where

$$\phi_c = (2\pi/d)(x\cos\theta + z_0 \sin\theta) \tag{7.49a}$$

$$\phi_t = (2\pi/d)\sin\theta a \cos\omega t \tag{7.49b}$$

By photographing this pattern with an exposure time much longer than the vibration period T, the resulting transmittance t of the film becomes proportional to $I(x,t)$ averaged over the vibration period. This is analogous to time-average holography (see Section 6.9) and gives for the transmittance

$$t = \frac{1}{T}\int_0^T I(x,y)\,dt = 2 + \frac{e^{i\phi_c}}{T}\int_0^T e^{i\phi_t}\,dt + \frac{e^{-i\phi_c}}{T}\int_0^T e^{-i\phi_t}\,dt \tag{7.50}$$

Now we have

$$\frac{1}{T}\int_0^T \mathrm{e}^{\pm \mathrm{i}\phi_t}\,\mathrm{d}t = \frac{1}{T}\int_0^T \exp[\pm i\,(2\pi/d)\sin\theta a\cos\omega t]\,\mathrm{d}t$$
$$= J_0\left(\frac{2\pi}{d}a\sin\theta\right) \tag{7.51}$$

which inserted into Equation (7.50) gives

$$t = 2\left[1 + J_0\left(\frac{2\pi}{d}a\sin\theta\right)\cos\phi_c\right] \tag{7.52}$$

where J_0 is the zeroth-order Bessel function. From this expression we see that the Bessel function amplitude modulates the fringe pattern on the static surface given by z_0. This is illustrated in Figure 7.9.

The negative with the transmittance given from Equation (7.52) can be placed in an optical filtering system in the same way as in the static case, resulting in an amplitude distribution in the image plane equal to

$$u = J_0\left(\frac{2\pi}{d}a\sin\theta\right)e^{\mathrm{i}\phi_c} \tag{7.53}$$

and hence an intensity distribution given by

$$I = J_0^2\left(\frac{2\pi}{d}a\sin\theta\right) \tag{7.54}$$

From the values of the arguments of the Bessel function corresponding to its maximum and zeros given on page 167, we find that light fringes occur when

$$a = \frac{d}{2\pi\sin\theta} \times [0, 3.83, 7.02, 10.17, \ldots] \tag{7.55a}$$

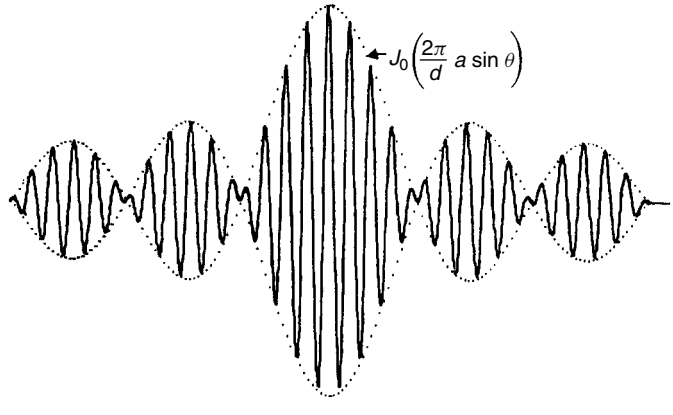

Figure 7.9

and dark fringes occur when

$$a = \frac{d}{2\pi \sin\theta} \times [2.40, 5.52, 8.65, 11.79, \ldots] \tag{7.55b}$$

The first dark fringe of this pattern thus corresponds to an amplitude a_l equal to

$$a_l = 0.38\frac{d}{\sin\theta} \tag{7.56}$$

which is a figure representing the sensitivity of the method.

7.5.4 Moiré Technique by Means of Digital Image Processing

A very convenient way of adding (subtracting) pictures is by means of digital image processing (Gåsvik 1983). A set-up for projection moiré is shown in Figure 7.10 where a grating is projected onto the object. The surface with projected fringes are imaged by a TV camera and the video signal is sent to an image processor, see Chapter 10. In this way it is possible to subtract a stored image from the image seen by the camera in real time. Figure 7.11 shows some examples of the results obtained with such a system. Figure 7.11(a) shows a cartridge casing with a dent. The reference image stored into the memory is taken from the undefective side of the casing. Figure 7.11(b) shows the result from two recordings of a 25-litre oil can before and after filling with water. In Figure 7.11(c) the system is applied to vibration analysis. It shows a circular plate centrally clamped to a shaft and excited by a shaker at a point in the lower right edge. The picture is a time-average recording resulting in a zeroth-order Bessel fringe function displaying the amplitude distribution of the plate as described in Section 7.5.3. For time-average recordings, the image processor is not necessary.

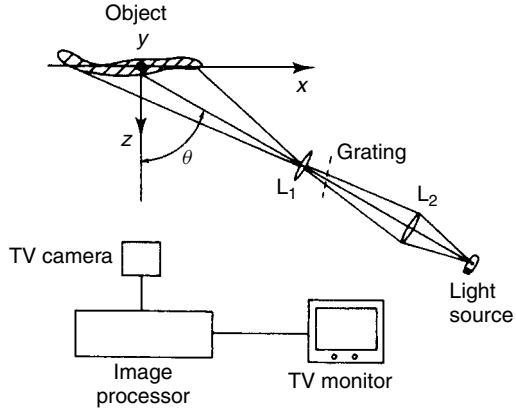

Figure 7.10 Projection moiré using TV-camera and digital image processor

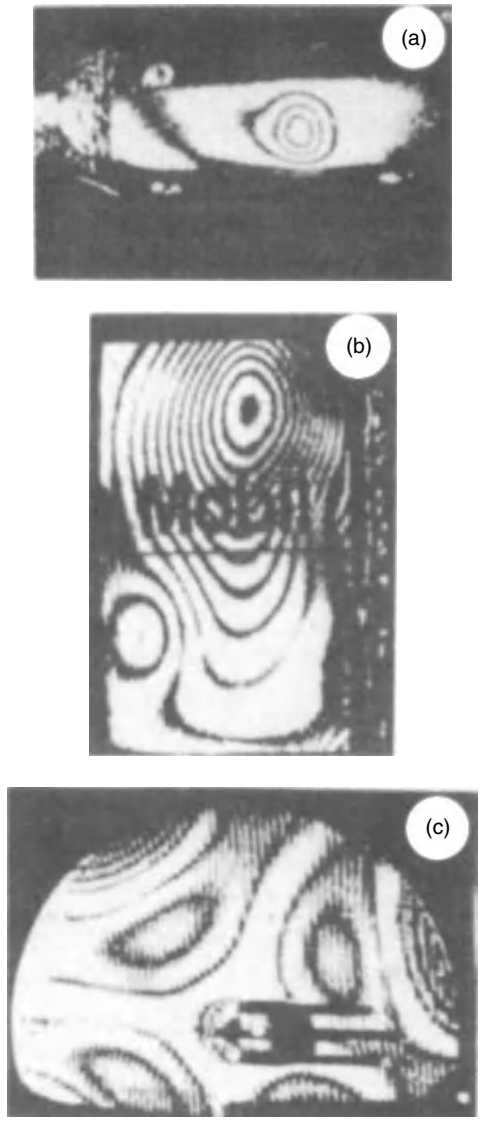

Figure 7.11 Examples of TV-moiré fringes: (a) cartridge casing with a dent. Contour interval 0.15 mm; (b) 25-litre oil can after filling with water; (c) time-average recording of a 400-mm diameter aluminium plate excited in the lower right edge. Frequency 250 Hz. Amplitude corresponding to the first dark fringe 0.16 mm

7.6 REFLECTION MOIRÉ

As we have already seen, moiré technique offers a wide variety of application methods. Most of them are, however, variations of the basic principles discussed in the preceding sections. Here we mention a method which to a certain extent differs from the previous

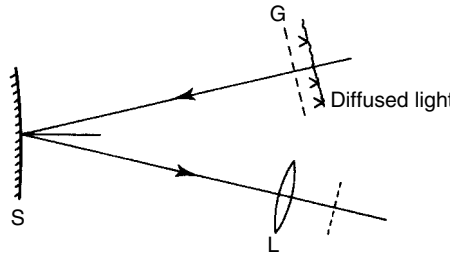

Figure 7.12 Reflection moiré

techniques. It is called Lichtenberg's method (Lichtenberg 1955) and can be applied on shiny, mirror-like surfaces and phase-objects (Liasi and North 1994).

Figure 7.12 shows the principle of the method. The smoothness of the surface S makes it possible to image the mirror image of the grating G by means of the lens L. As in previous methods, a grating can be placed in the image plane of L or the mirror image of G can be photographed before and after the deformation of S. The result is a moiré pattern defining the derivative of the height profile, i.e. the slope of the deformation.

In an analysis of the resolution of the reflection moiré method it is found that the maximum resolution that can be obtained with a viewing camera is of the order 7×10^{-3} radians.

7.7 TRIANGULATION

Shadow moiré and projected fringes are techniques based on the triangulation principle. We close this chapter by considering a simple triangulation probe. In Figure 7.13 a laser beam is incident on a diffusely scattering surface under an angle θ_1. The resulting light spot on the surface is imaged by a lens onto a detector D. The optical axis of the lens makes an angle θ_2 to the surface normal. Assume that the object moves a distance s normal to its surface. From the figure, using simple trigonometric relations, we find that

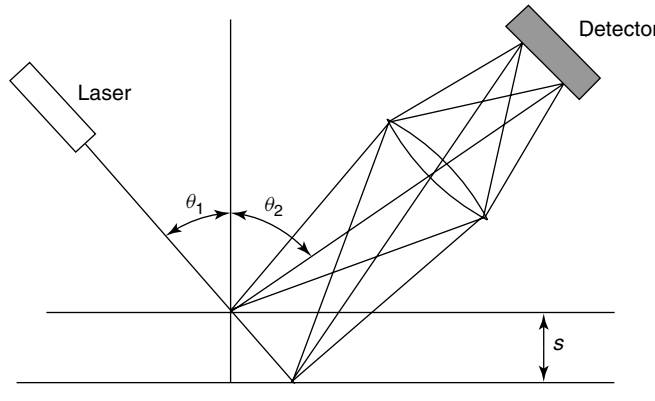

Figure 7.13 Triangulation probe

the corresponding movement of the imaged spot on the detector is given by (see Eq. 7.21)

$$s' = m\frac{s\sin(\theta_1+\theta_2)}{\cos\theta_1} = ms(\tan\theta_1\cos\theta_2+\sin\theta_2) \tag{7.57}$$

where m is the transversal magnification of the lens. The detector is position-sensing, i.e. it gives an output voltage proportional to the distance of the light spot from the centre of the detector. It is the centroid of the light spot that is sensed and thus the position measurement is independent of the spot diameter as long as it is inside the detector area. Therefore sharp focusing is not critical. The position of an unexpanded laser beam directly incident on such a detector can be determined to an accuracy of less than 1μm. From Equation (7.57) we see that the movement s' can be magnified by the lens, thereby increasing the sensitivity. However, the size of the light spot will also be magnified, and this must always lie inside the detector area to avoid measurement errors, thus limiting the usable magnification.

In many applications, θ_1 is set to zero. Then very precise measurements of movements along the light beam (the z-axis) can be made. Since the light spot is then always on the z-axis, it is a good idea to tilt the detector such that the spot is always focused on the detector. To make measurements on small details, the diameter of a laser beam might be too large. Then clever optics forming a thin beam through the measurement volume have to be constructed and light sources other than lasers might be a better alternative. Such probes can be used to measure the profile of screws and other small parts, for example.

PROBLEMS

7.1 Two gratings with amplitude transmittance

$$t(x, y) = a\left[1+\cos\left(\frac{2\pi}{p}x\right)\right]$$

are laid in contact with an angle α between the grating lines. Calculate $t_1 \cdot t_2$.

7.2 A circular zone plate with centre at (x_0, y_0) has an amplitude transmittance given by

$$t(x, y) = \tfrac{1}{2}\{1+\cos\beta[(x-x_0)^2+(y-y_0)^2]\}$$

where β is a constant. Suppose that two zone plate transmittances are laid in contact with a displacement d between their centres.

(a) Show that the resulting moiré fringes describes a new zone-plate pattern.

(b) Find the centre and the frequency of this new zone plate pattern.

7.3 We attach a grating of period p to a bar, whereafter the bar undergoes a uniaxial tension resulting in a strain equal to ε_x.

(a) Write down the transmittances t_1 and t_2 of the grating before and after the load.

(b) Find an expression for $t_1 + t_2$ describing the moiré pattern.

(c) If $\varepsilon_x = 10^{-3}$, the grating frequency is 20 lines/mm and the length of the bar is 10 cm, how many moiré fringes are observed?

7.4 In shadow moiré, the reference grating t_1 is multiplied by the object (shadow) grating t_2. In what sense can we say that this is a sort of synchronous demodulation of t_2? What is the low-pass filter in this case?

7.5 Consider the method of projected fringes using interference between two plane waves (Figure 7.6(a)). Assume that the camera is looking normal to the surface from infinity (i.e. $\theta_2 = 0$).

(a) calculate the out-of-plane displacement Δz per fringe in this case.

(b) Based on pure geometric considerations, there is a limit to the sensitivity (displacement per fringe) in this set-up. Find this limit and the corresponding values of θ_1 and α (the angle between the two plane waves).

(c) Using $\lambda = 600$ nm, calculate the mean spatial frequency in lines/mm on the surface in this case. Why is this measuring sensitivity unattainable?